SEISMIC RESPONSE AND ENGINEERING OF COLD-FORMED STEEL FRAMED BUILDINGS

B.W. Schafer[1], D. Ayhan[2], J. Leng[3], P. Liu[2], D. Padilla-Llano[4], K.D. Peterman[3], M. Stehman[3], S.G. Buonopane[5], M. Eatherton[6], R. Madsen[7], B. Manley[8], C.D. Moen[9], N. Nakata[10], C. Rogers[11], C. Yu[12]

* Johns Hopkins University, Baltimore, Maryland USA
e-mail: schafer@jhu.edu

Keywords: Cold-formed steel, seismic response, earthquake engineering, performance-based design.

Abstract. *Buildings framed from cold-formed steel members are becoming increasingly common. Significant research has been conducted on individual cold-formed steel members, but little research has been done on full buildings framed from cold-formed steel. In the past, testing on individual shear walls has been used to provide insights and create safe seismic designs for cold-formed steel buildings, but understanding and modeling of whole buildings has been out of reach. As a result, seismic performance-based design has also remained out of reach for cold-formed steel framed buildings. Recently, a North American effort under the abbreviated name: CFS-NEES has begun to address this challenge. Major deliverables in the CFS-NEES effort include: shear wall testing, characterization, and modeling; cyclic member testing, characterization, and modeling; and, whole building shake table testing, and modeling. The research provides the necessary building blocks for developing efficient nonlinear time history models of buildings framed from cold-formed steel. In addition, the experiments demonstrate the large difference between idealized engineering models of the seismic force-resisting system and the superior performance of the full building system.*

1 INTRODUCTION

After the Second World War, the United States was left with a tremendous amount of excess sheet steel capacity. Cold-formed steel framing came into being as a means to take advantage of the economy and efficiency of using lightweight structural members. In North America, nonstructural cold-formed steel members now lead the construction market for

[1]Professor, Johns Hopkins University, <schafer@jhu.edu>

[2]Visiting Student Scholar, Johns Hopkins University

[3]Graduate Research Assistant, Johns Hopkins University

[4]Graduate Research Assistant, Virginia Polytechnic and State University

[5]Associate Professor, Bucknell University

[6]Assistant Professor, Virginia Polytechnic and State University

[7]Senior Project Engineer, Devco Engineering

[8]Regional Director, American Iron and Steel Institute

[9]Associate Professor, Virginia Polytechnic and State University

[10]Assistant Professor, Johns Hopkins University

[11]Professor, McGill University

[12]Associate Professor, University of North Texas

interior partition walls and curtain walls. For structural applications, cold-formed steel has long been used as the secondary system for purlins and girts in metal buildings, and for industrial storage racks, including, on occasion, even rack-supported buildings. However, the use of cold-formed steel as the primary structural members in buildings has undergone a slower adoption process. Initially focused on residential construction, and mimicking wood construction, cold-formed steel framing has experienced only modest levels of adoption in North America and beyond.

Today, structural cold-formed steel framing systems are focused on mid-rise structures with two primary construction methods demonstrating success in the market: (1) efficient on-site or remote-site fabrication methods, and (2) panelized systems. Framecad is an example of company that provides turn-key systems for on-site construction, even in remote locations. Using a small automated roll-forming machine and steel coils, all members are manufactured on-site. The result is a complete cold-formed steel framed building, as shown in Figure 1-(a). Framecad structures utilize small built-up trusses more often than other, more traditional, cold-formed steel framing systems, but these structures have demonstrated the potential of cold-formed steel framed buildings to work in a wide variety of markets. In contrast, ClarkDietrich Building Systems is an example of a company that partners with a U.S. roll-former; uses standard shapes (in the U.S. these are designated in [1] with manufacturers providing additional specifics, as needed); and, then with Building Information Models and efficient panelization software, details and fabricates large wall panels in the factory shipping them directly to the building site. The result, such as Figure 1(b), is a rapidly constructed structure that uses cold-formed steel framing throughout.

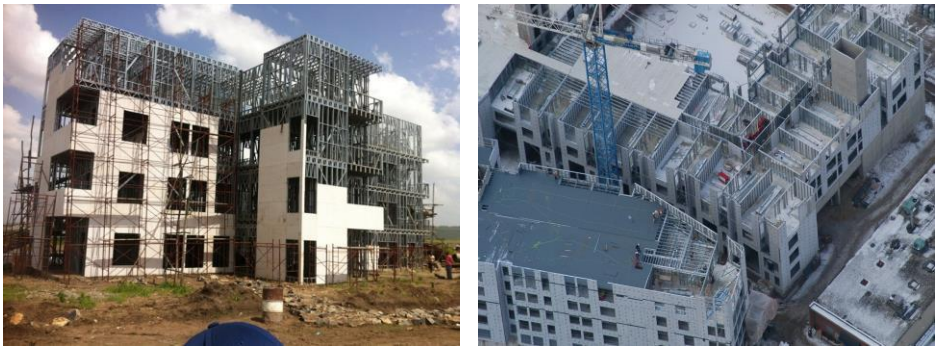

(a) construction by Framecad in North Africa (b) construction by ClarkDietrich Building Systems in USA

Figure 1: Examples of contemporary cold-formed steel framed buildings

As cold-formed steel framing becomes more prominent in building design, it has become necessary to develop full building solutions. Component level design has been available in codes and standards around the world [2,3] for some time, but lateral force resisting systems were relatively ad hoc until the modern era. The recent push towards multi-story construction, in particular, has required developing specific full building solutions for cold-formed steel. Seismic performance of cold-formed steel framed buildings enjoys the potential benefit of using a lightweight solution, thus minimizing the seismic mass, compared with conventional masonry or concrete construction. However, the performance of seismic force-resisting systems framed from, or compatible with, cold-formed steel members was relatively unknown

until the last 20 years. Since then, significant research has been conducted to advance the state of the art in that time.

In North America, the seminal work of Serrette and colleagues (e.g., [4]) provided characterization of cold-formed steel framed, wood sheathed, shear wall panels that were codified [5] and formed the basis for lateral force resisting systems framed from cold-formed steel members. Building on this foundation, Rogers and colleagues expanded the scope for cold-formed steel framed, wood sheathed, shear wall panels [6] as well as developed experimental performance and understanding for cold-formed steel framed steel strap walls [7],steel sheet sheathed shear walls [8], and multi-story shear wall details [9]. Rogers' work along with additional testing by Yu on steel sheet sheathed shear walls [10] was codified in North America [5].

In Europe, multi-year efforts in Italy and Romania stand out as contributing to the state of the art. To assist in filling the design gap in Italy, Landolfo and colleagues performed cold-formed steel framed, wood sheathed, shear wall tests [11], fastener testing [12], prototype structures [13], and complete design philosophies [14]. Dubina and colleagues performed cold-formed steel framed, wood and plaster sheathed, shear wall tests [15], complementary numerical models [16], and also developed full seismic design procedures [17].

Though generally not seismically active, the early adoption of cold-formed steel framing in low-rise (primarily residential) construction in Australia also led to useful experimental and full-scale response results on cold-formed steel framed structures [18]. Recent growth in China has created additional research in this area, particularly experimental efforts [19]. Today, research is active in the following areas: development of novel shear walls; developing system-level understanding necessary for mid-rise cold-formed steel framed construction; developing guidance for floor and roof diaphragm behavior appropriate for cold-formed steel framing; and generally expanding our knowledge and abilities in modeling full building/system seismic response. Codes and standards for cold-formed steel seismic design continue to advance as well [20].

In the last 4 years, the author has led a new North American effort to advance our understanding of cold-formed steel framed buildings in seismic events. Funded by the U.S. National Science Foundation (NSF) and the American Iron and Steel Institute, the work was formally a part of the NSF Network for Earthquake Engineering Simulation (NEES) research program under the project title: Enabling Performance-Based Seismic Design of Multi-Story Cold-Formed Steel Structures, or in short CFS-NEES. The objective of CFS-NEES was to develop understanding and advance modeling towards seismic performance-based design of cold-formed steel framed buildings. The CFS-NEES effort had as a central focus full-scale shake table testing and related modeling of a cold-formed steel ledger-framed building with wood structural panel shear walls and floors.

This paper summarizes the CFS-NEES research effort. The research spanned from small-scale tests on fasteners to full-scale tests on buildings and included simulation, modeling, and the development of design guidance across these same scales. The ultimate objective was to provide all the necessary building blocks to advance simulation tools for seismic performance-based design evaluations of cold-formed steel framed buildings. Section 2 introduces the CFS-NEES archetype building that was utilized for full-scale testing and related modeling; unique details of the building are highlighted. Section 3 summarizes experimental work to characterize the cyclic performance of cold-formed steel framing members in compression and bending; this data is currently unavailable and a significant impediment to building comprehensive and efficient models. Section 4 includes the shear wall testing conducted specifically to address the details in the CFS-NEES archetype building.

Section 5 provides the CFS-NEES specific project additions to the experimental database on frame-fastener-sheathing cyclic performance; this is the key energy dissipating mechanism in cold-formed steel framed, wood sheathed, shear walls. Section 6 briefly discusses modeling cold-formed steel shear walls and introduces recent CFS-NEES advances in shear wall modeling that utilize connection data to provide a robust tool for developing predictions of shear wall performance appropriate for use in simulations and design. Section 7 details the full-scale shake table tests of the CFS-NEES archetype building, emphasizing the system performance of cold-formed steel framed buildings. Section 8 summarizes the wide breadth of modeling that has been conducted on the CFS-NEES archetype building, and explores the relationship between model fidelity and prediction of building response. Finally, Section 9 examines future needs in seismic earthquake engineering for buildings framed from cold- formed steel.

2 CFS-NEES BUILDING ARCHETYPE

Central to the CFS-NEES effort was the professional design of a two-story commercial building framed from cold-formed steel. The building is sited in Orange County, CA (site class D) and is 15.2 m (49 ft – 9 in.) x 7.0 m (23 ft) in plan and 5.9 m (19 ft – 3 in.) tall with a total seismic weight of 347 kN (78 kips). The design was completed by Madsen of Devco Engineering, with input from the project team and the Industrial Advisory Board (see acknowledgments). A design narrative, complete calculations, and full drawings are available for the building [21,22]. The building utilizes cold-formed steel framed, OSB-sheathed shear walls for the seismic force-resisting system. Cold-formed steel joists with OSB-sheathing are detailed for the floor and roof diaphragm.

A key feature of the building was the selection and use of ledger framing, a choice that was strongly advocated for by the Industrial Advisory Board based on current practice. In ledger framing, the building is constructed one floor at a time, but the floor joists are hung from the top of the studs. The joists and studs are not necessarily aligned so a ledger, or carrier track, is attached to the interior face of the studs running along the length of the wall to provide a connection point for the joists, as shown in Figure 2. A key detail in this system is the joining of the shear wall chord studs across stories, illustrated in Figure 2b: a flat plate attached to the stud web penetrates through the floor. sheathing and wall tracks. Another notable feature of ledger framing is that the floor sheathing runs through to the edge of the building and is attached directly to the top track of the walls, as shown in Figure 2b.

(a) rendering from BIM model, only shear walls and

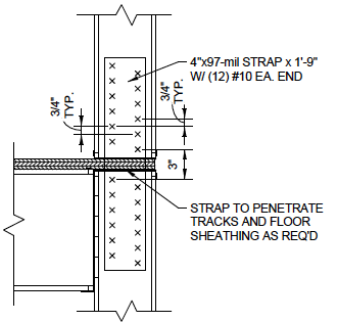

(b) detail at shear wall chord stud

diaphragms sheathed

Figure 2: CFS-NEES archetype building utilized to organize research and for full-scale testing

3 CFS-NEES MEMBER CHARACTERIZATION

Fundamental to the behavior of thin-walled cold-formed steel members is the stiffness reductions that may occur due to local, distortional, and global buckling under load. These reductions must be captured within designs and models if the full system created by cold-formed steel members is to be assessed. Using existing test data, a new method was developed for determining the stiffness reduction and backbone moment-rotation and/or moment-curvature response under local and distortional buckling [23, 24, 25, and 26]. The method is general, and, in the spirit of the Direct Strength Method of cold-formed steel design, uses the cross-Section slenderness to predict the reduced stiffness and full backbone response.

Given a lack of available data on member cyclic response, the American Iron and Steel Institute in collaboration with CFS-NEES funded a project to characterize the cyclic response of cold-formed steel members. The research completed at Virginia Tech investigated the cyclic response of thin-walled cold-formed steel members with carefully selected boundary conditions subjected to cyclic axial and bending loads [**27-32**]. The results summarized in [**31**] highlight the energy dissipation capabilities and post-buckling strength and stiffness of CFS members and shows that these are a function of the cross-section slenderness (e.g. Figure 3). These results form the basis for development of seismic force-resisting systems that incorporate complete cold-formed steel member response, as opposed to current systems, that largely seek to use alternative mechanisms, independent from the members (bearing in wood or steel connections, yielding of straps, etc.), to resist seismic demands.

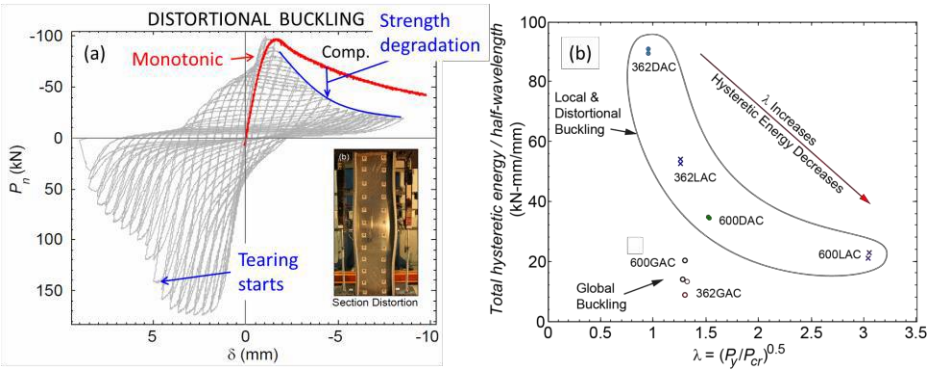

Figure 3. (a) Cyclic load-deformation response in distortional buckling for 600S137-54, and (b) total hysteretic energy dissipation variation with slenderness for all axial members tested, see 31]

4 CFS-NEES SHEAR WALL CHARACTERIZATION

The CFS-NEES archetype building employs cold-formed steel framed, OSB-sheathed, shear walls. This is a common shear wall type, available in AISI S213 [5] for prediction of its strength and stiffness. However, actual construction differs from the tests used to develop the

AISI-S213 tables: shear wall sizes are often not equal to the standard 1.2m x 2.4 m (4 ft x 8 ft) OSB panel, so numerous additional horizontal and vertical seams were present in the actual shear walls; a large 2.5 mm (0.097 in.) thick 305mm (12 in.) deep carrier or ledger track blocks out 205 mm (12 in.) at the top of a shear wall; the interior face of the wall is sheathed with gypsum board; and, in some cases, the field studs differ in thickness to the chord studs that frame out the shear wall. Additionally, complete hysteretic response of these shear walls is not available. As a result, a test program and characterization effort was initiated.

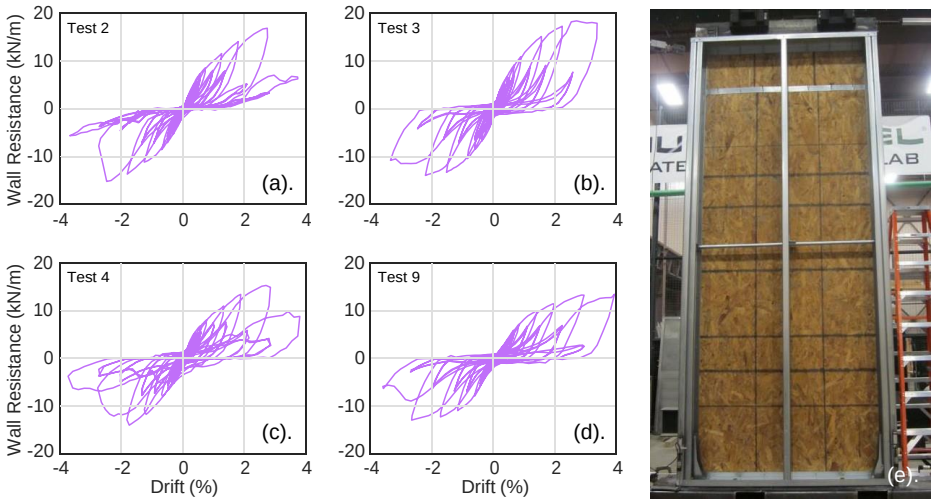

Figure 4. Hysteretic response of 1.22 m x 2.74 m OSB sheathed shear walls (a) with ledger, (b) and gypsum board, (c) baseline, and (d) extra vertical seam (e) rear of Test 4

(Collaborating with co-author Yu at with the University of North Texas, the project team was able to efficiently test 15 OSB-sheathed shear walls which were specifically designed for the CFS-NEES building.) Thanks to a collaborative effort with the University of North Texas, the CFS-NEES project was able to efficiently test 15 OSB-sheathed shear walls. Testing following the CUREE protocol, and typical response of 1.2 m x 2.7 m (4 ft x 9 ft) shear walls are provided in Figure 4, with complete results available in the test report [27] and related papers [28, 29]. Strength degradation initiated at levels between 2% and 4% drift. Developed strength was in excess of AISI-S213 predictions, except in the case where shear wall field studs are thinner than the chord studs, a common practice for lightly loaded upper stories that should be accounted for in design. The addition of panel seams, ledger, and interior gypsum cause some divergence in stiffness predictions from AISI-S213 and can lead to greater than expected overstrength.

5 CFS-NEES "FASTENER" CHARACTERIZATION

For cold-formed steel framed OSB-sheathed shear walls the key energy dissipating mechanism occurs at the stud-fastener-sheathing connection. As the studs rack laterally the fasteners tilt (and bend) as they bear into and damage the sheathing. Stiffness of the shear walls also relies on this same mechanism. In shear walls framed and sheathed from wood, it

has been found that a similar mechanism dominates the response and reasonable estimates of shear wall parameters can be derived directly from this local "fastener" response [30].

To characterize this "fastener" response, a series of cyclic tests on stud-fastener-sheathing assemblies, consistent with the CFS-NEES building details, as depicted in Figure 5a,b were conducted. The tests varied stud thickness, fastener spacing, and sheathing type. Typical force-deformation results are provided in Figure 5c; the direct shear response of the fastener assemblies is similar to the full walls, but even more pinched. Each test was characterized using the Pinching04 model [31], and complete results are provided in a CFS-NEES research report [32] and a related paper [33]. Section 7 discusses connecting the fastener response to the overall shear wall response and the results indicate that small-scale fastener tests have excellent predictive power for full-scale shear wall tests.

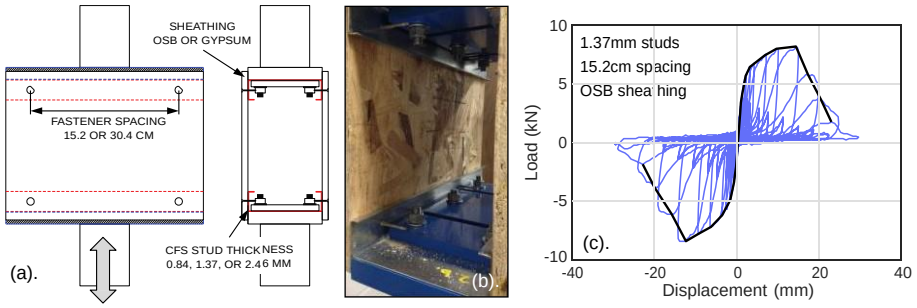

Figure 5. Fastener testing assembly (a) front, and side detail, (b) photograph of test specimen and (c) typical hysteretic response with backbone

A lack of knowledge on the stiffness and cyclic response of typical connections in cold-formed steel goes beyond the details common in shear walls. As a result, as a companion to the CFS-NEES effort, an extensive project was undertaken at Virginia Tech to more fully understand the cyclic response of cold-formed steel connections [34]. The work is currently ongoing. The results provide a key building block for models of cold-formed steel assemblages and full buildings.

6 CFS-NEES SHEAR WALL MODELING

Shear walls provide a key element in seismic resistance and thus are a major focus of any simulation effort. For the CFS-NEES archetype building, our own direct testing is available in addition to guidance from codes and specifications. For efficient building models, a one-dimensional (V-Δ) phenomenological model is a useful approximation of a shear wall. This may be implemented as a shear spring, or converted to an equivalent truss – regardless, a single degree of freedom approximation to shear walls is a highly desired first step.

Characterization of the CFS-NEES shear wall test results (Section 4) was completed by determination of parameters for one-dimensional (V-Δ) equivalent energy elastic-plastic (EEEP) model and a Pinching04 model [36]. EEEP models are not appropriate for time-history analysis of these systems, only for pushover analysis. The Pinching04 models provide the ability to have a multi-linear backbone curve with cyclic degradation and pinching and are able to capture the key features of the shear wall response (i.e. details of Figure 4) and are utilized directly in the CFS-NEES building models of Section 8.

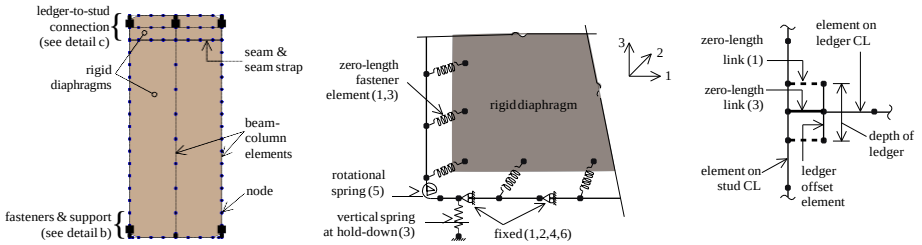

(a) Typical mesh. (b) Detail of fasteners and supports. (c) Detail of ledger-to-stud connection.

Figure 6: Example computational Model: (a) full wall, (b) base and fastener details, and (c) ledger track details

In many cases, due to shear wall size, fastener schedule, sheathing type, framing details, etc. it is not possible to directly use the codified and prescriptive shear wall details provided, e.g. in AISI-S213 [5]. In this situation, the primary recourse for the engineer is to simplify ortest. For wood-sheathed shear walls, since the nonlinearity at the stud-fastener-sheathing connection dominates response, use of small-scale fastener tests in combination with a computational model to predict full-scale shear wall response [31,35,36] has been explored. The basic model, depicted in Figure 6, models the cold-formed steel framing as beam elements, each fastener location with a nonlinear (Pinching04) spring, and the sheathing itself either as a rigid or flexible diaphragm. The resulting model is computationally efficient and capable of accurately predicting full-wall response even in degrading cycles, e.g. see Figure 7. The model also provides a means to better understand the shear wall behavior, e.g. Figure 8, and is now being used by the research team to explore system reliability and wall system (shear wall plus gravity wall) modeling [43]. In addition, the cyclic experimental and characterization work of Section 3 may also be incorporated into these models [31,37] such that chord stud buckling limit states may be captured in these models as well, e.g., Figure 9. The goal of this work is to provide a computational tool for engineers that can be used to augment the prescriptive shear wall tables in current use, while at the same time providing a tool that can predict full hysteretic response for engineers pursuing seismic performance-based design of these systems in the future. Current work has advanced well towards this goal.

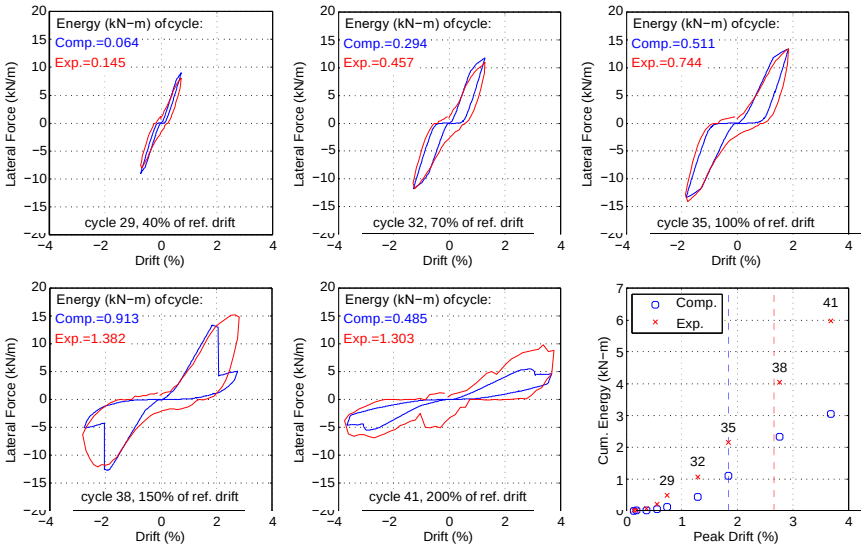

Figure 7: Example (Model 4 of [36]) load-displacement response for five peak cycles and cumulative hysteretic energy dissipation.

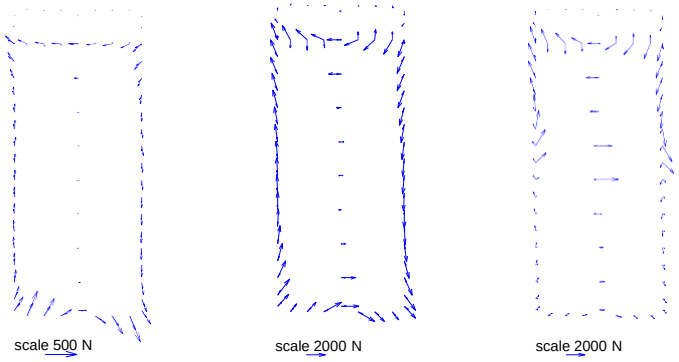

Figure 8: Vector force diagrams of fastener forces in Model 3 of [36] at three different levels: (a) elastic (1.9 kN/m), (b) peak lateral force (17.5 kN/m), (c) peak lateral displacement (10.9 kN/m).

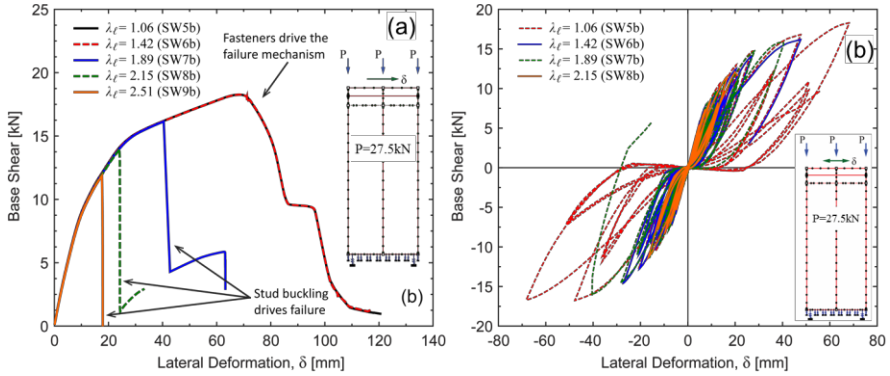

Figure 9. Shear wall response including local buckling in vertical members. The figure shows the sensitivity of the response to the vertical member cross-section slenderness for (a) monotonic loading and (b) reverse cyclic push-over loading, see [31]

7 CFS-NEES FULL SCALE BUILDING TESTING

Full-scale testing of the CFS-NEES archetype building was conducted in the Summer of 2013 at the NEES shake table facility at the University of Buffalo [38]. The testing was conducted in two primary phases: Phase 1 and 2, as shown in Figure 10. The Phase 1 building was the complete structural system and represents the engineered building system both for lateral and gravity loading. Significant supplemental mass was added—over four times the building self-weight—to meet code specified [21,39] gravity load levels. The Phase 1 building was tested through the three-axis Canoga Park record (16%, 44% and 100% levels) from the 1994 Northridge earthquake. At 100% scale this is essentially equal to the Design Basis Earthquake (DBE) per U.S. standards [21,~~44~~].

The Phase 1 building was deconstructed subsequent to the 100% Canoga Park testing and a new building constructed to the same specifications, Phase 2, was built on the shake tables.

The Phase 2 structure continued construction past the engineered system. As depicted in Figure 11, in Phase 2b the gravity exterior walls were externally sheathed, in Phase 2c the interior face of the exterior walls were sheathed with gypsum, in Phase 2d all the interior partition walls and staircases were installed, and finally in Phase 2e (also see Figure 10b) exterior DensGlass was installed.

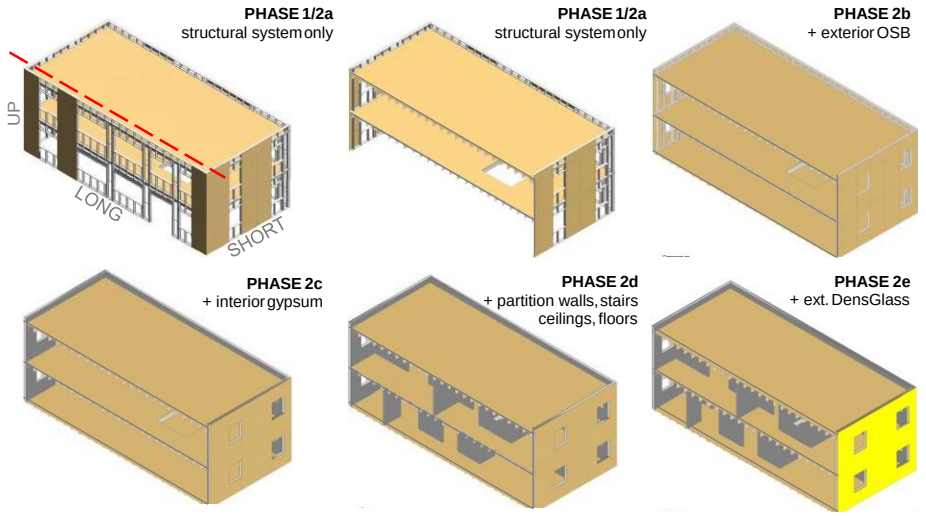

Figure 11: Illustration of construction milestones within Phase 2 testing, shown via cross Section views of building specimens (dashed line indicates location of cross Section)

Throughout the construction phases the total mass was held constant by adjusting the supplemental mass in the structure. The Phase 2 structure was subjected to low level excitation tests and system identification testing during the construction phases. Finally, the Phase 2e building was subjected to the 100% Canoga Park record, and then to the three-axis near-field Rinaldi record at 100%, also from the 1994 Northridge earthquake. For this structure, 100% Rinaldi is consistent with the Maximum Credible Earthquake (MCE) per U.S. standards.

The stiffness, damping, and response of the building is significantly altered by the non-structural systems. Figure 12 provides the decrease in the first mode period of the building as determined from system identification tests in the long and short directions of the building through the Phase 2 construction. Comparing Phase 1/2a to Phase 2e, the long direction first mode period decreases from 0.32 s to 0.15 s, given constant mass, this represents a 4.5 times increase in the building stiffness. (The short direction experiences a 1.9 times increase in stiffness). Based on 0.1 g white noise-driven system identification testing, damping is measured at 4% prior to Phase 1 testing, and 9% prior to Phase 2e testing. Subsequent to the 100% Canoga Park record, damping is measured at 18% on the Phase 1 building, and subsequent to the 100% Rinaldi record, damping is measured at 15% on the Phase 2e building.

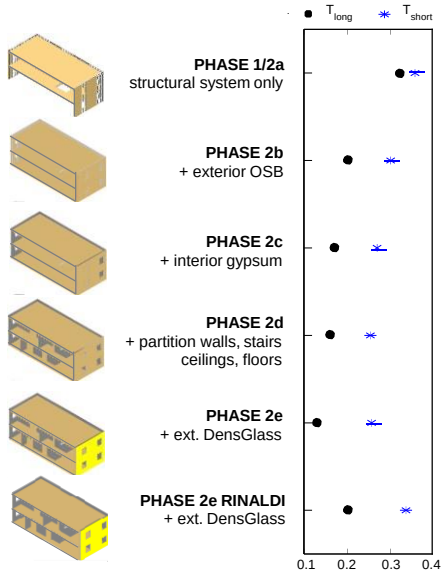

Figure 12. Shift in long and short direction first mode period through construction phases

Response of the building during testing was captured by an extensive sensor array [38]. Story drift of the Phase 1 building during the 100% Canoga Park excitation in the long (u) direction and short (v) direction for the first (subscript 1) and second (subscript 2) stories of height, h, are provided in Figure 13. A peak first storydrift of 1.18% is recorded. This maybe compared with the story drift in the tested CFS-NEES shear walls in Figure 4. Recorded peak story drift for a sample of the Phase 1 and Phase 2 testing is provided in Table 1. Phase 1, 100% Canoga Park, is the maximum experienced story drift in the testing. Phase 2e testing with the 100% Rinaldi excitation increases the ground motion lateral S_a from 0.42 g to 0.83 g, but the experienced peak story drift is only 0.72%. (It should be noted that 100% Rinaldi also includes a vertical S_a of 0.82 g that due to difficulties in table tuning resulted in a 1.27 g peak during testing).

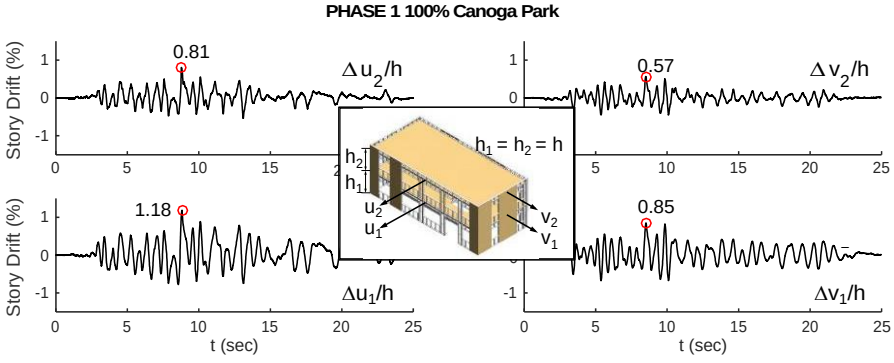

Figure 13: Drift percent for Phase 1 building under the 100% Canoga Park ground motion

Table 1: Maximum percent story drift across phases and ground motions

		MAX % STORY DRIFT (Δ/h)			
		LONG		**SHORT**	
Phase	**Ground Motion**	**$\Delta u_1/h$**	**$\Delta u_2/h$**	**$\Delta v_1/h$**	**$\Delta v_2/h$**
-	-	%	%	%	%
1	44% Canoga Park	0.55	0.38	0.36	0.29
2b	44% Canoga Park	0.19	0.29	0.11	0.21
2c	44% Canoga Park	0.12	-0.22	0.11	0.17
2d	44% Canoga Park	0.11	-0.19	0.08	-0.15
2e	44% Canoga Park	0.08	-0.20	0.06	-0.14
1	100% Canoga Park	1.18	0.81	0.85	0.56
2e	100% Canoga Park	0.25	-0.48	0.16	-0.32
2e	16% Rinaldi	0.11	0.07	-0.16	0.11
2e	100% Rinaldi	0.67	-0.72	0.45	0.49

Pre-compressed load cells were installed on the anchor rods at the shear wall hold down locations. These sensors provide a means to understand how the building, and the shear walls in particular, carry the seismic demands. Figure 14 provides a summary of the building displaced shape along with the hold down response at peak drift during testing. Note, the load cell can read tension and a small amount of compression (only up to the amount of pre-tension on the anchor rods) therefore tension may be read based on magnitude (length of the bar), and compression is essentially only an indicator of compression, not its magnitude. The response is complex. The building is designed as a series of independent shear walls and assuming a flexible diaphragm. Under these assumptions, each shear wall should experience force couples of tension and compression; however, the actual response is more tied to the overall motion of the building (in three dimensions) and significant amount of coupling amongst shear walls is observed. Comparison of 100% Canoga Park in the Phase 1 and Phase 2e response in the lower left of Figure 14 provides further evidence that the engineered system (Phase 1) and the actual building (Phase 2e) do not respond the same.

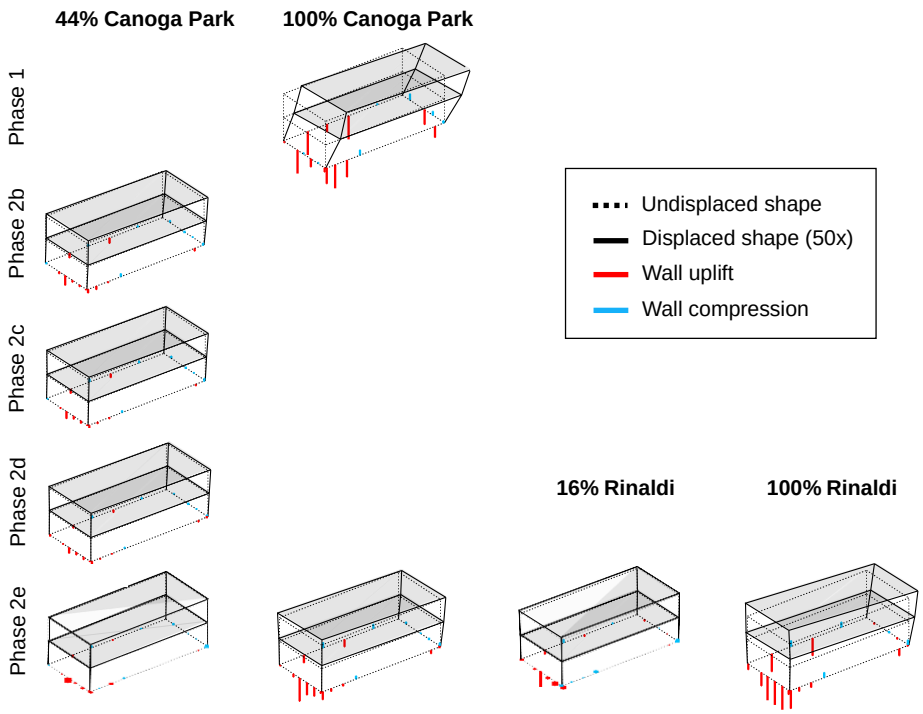

Figure 14: Shear wall anchor forces superimposed on the deformed and undeformed shapes of the building specimens at peak first story drift in the long direction

Under seismic testing both the Phase 1 and Phase 2e buildings experienced minimal drift and returned to straight after excitation. For the Phase 2e building, the story drift under Rinaldi was less than 1% and damage only occurred in the interior non-structural walls, largely confined to corners near openings, as photographed in Figure 15. This full scale testing provides a first examination of the full system effect for buildings framed from cold-formed steel and it is significant: the building is stiffer and stronger than engineering designs suggest; the building responds as a system, not as a set of uncoupled shear walls; and the gravity system contributes to the lateral response.

Figure 15: (a) Phase 2e specimen post-test (b) drywall cracking at interior window corner (c) drywall cracking and crushing at interior partition wall base (d) drywall cracking at interior window corners (location of cracks are encircled)

8 FULL SCALE BUILDING MODELING

The CFS-NEES full scale building modeling effort has two major goals: (1) to provide a model that can meaningfully predict the CFS-NEES building response in order to better understand the behavior of the building and use the model to examine response against a full suite of seismic excitations, and (2) to evaluate what level of model fidelity is necessary for engineers and researchers modeling buildings framed from cold-formed steel. All of the full-scale building modeling is implemented in OpenSees. Modeling the response of cold-formed steel buildings, even a particular cold-formed steel building, introduces an enormous number of potential assumptions. A complete model tree spanning from two-dimensional models with strength and stiffness based on specifications available to engineers, e.g. [5], to three-dimensional models with shear walls based on direct experimental characterization and all steel framing explicitly modeled are all explored.

A truncated version of the model tree is provided in Table 2, see [40] for the complete version and for all modeling details. Two basic classes of model are explored: (1) state-of-the practice, or "P" models, and (2) state-of-the art, or "A" models. The P models use shear wall stiffness and strength based on codes and standards, i.e. AISI S213, and ignore the lateral contribution from all elements except the shear walls. For nonlinear hysteretic models, the P

models use either EPP or a simplified Pinching4 model as described in [40]. The P models are generally 2D, but 3D models are also created and appear as depicted in Figure 16a. The A models provide an exploration of various state-of-the-art representations of the full CFS-NEES building. Stiffness and strength in the A models are based on direct testing or higher-fidelity surrogate models. In most A models, the gravity framing is explicitly included – this requires greater sophistication in the shear wall modeling as well, resulting in a typical model as provided in Figure 16b. The A models also explore the impact of the diaphragm stiffness on the response.

Table 2: Modeling options of CFS-NEES archetype building

			State of the Practice				State of the Art										
							Phase 1/Phase 2a					Phase 2b			Phase 2c			Phase 2d
Component	Property	Option	P-2D-a	**P-2D-b**	P-3D-RD-a	**P-3D-RD-b**	**A1-2D-a**	**A1-3D-RD-a**	A1-3D-RD-b	A1-3D-RD-c	**A1-3D-SD-a**	A2b-2D-a	**A2b-3D-RD-a**	**A2b-3D-SD-a**	A2c-2D-a	**A2c-3D-RD-a**	**A2c-3D-SD-a**	**A2d-3D-RD-a**
Shear wall	Stiffness	$K(0.4V_{nP})$	X	X	X	X												
		$K(V_{nP})$					X	X		X	X	X	X	X	X	X	X	X
		$K(0.2V_{nA})$							X									
		$K(0.4V_{nA})$					X	X	X	X	X	X	X	X	X	X	X	X
	Capacity	V_{nA}																
		V_{nP}	X	X	X	X												
	Backbone	EPP	X		X													
		Pinching4		X		X	X	X	X	X	X	X	X	X	X	X	X	X
	Panel size	Whole	X	X	X	X				X								
		Subpanels					X	X	X		X	X	X	X	X	X	X	X
Hold-down	General	Smeared	X	X	X	X												
		Discrete					X	X	X	X	X	X	X	X	X	X	X	X
Shear anchors	General	Ignored	X	X	X	X												
		Included					X	X	X	X	X	X	X	X	X	X	X	X
Diaphragm	Stiffness	Flexible	X	X			X					X			X			
		Rigid			X	X		X	X	X			X			X		X
		Semi-rigid									X			X			X	
	Pinching	None	X	X	X	X	X	X	X	X		X			X			X
		Pinching4									X		X	X		X	X	
Gravity exterior walls	General	None	X	X	X	X												
		Frame					X	X	X		X							
		Full										X	X	X	X	X	X	X
Gypsum sheathing	General	Ignored	X	X	X	X	X	X	X	X	X	X	X	X				
		Included													X	X	X	X
Interior walls	General	Ignored	X	X	X	X	X	X	X	X	X	X	X	X	X	X	X	
		Included																X
Mass distribution	General	Corner	X	X	X	X	X			X		X			X			
		Stud ends						X	X		X		X	X		X	X	X

*Shaded columns with bold type indicate that the specific model is addressed in this paper other models and full details in[40]

As reported initially in [41,42] and detailed in [40], a surprisingly high degree of model complexity is required for developing observed system response. Consider the model of Figure 16a: 3D with only shear walls modeled (rigid diaphragm), i.e. model P-3D-RD-b. The first translational mode period of this shear wall only model is 0.66 s (in the short direction). Different from reality, the P model's torsional mode period is even larger. The same building (with only shear walls sheathed, aka Phase 1) in white noise testing has a first mode period of 0.36 s (in the short direction). An alternative model, with all wall framing explicitly included (A1-3D-RD-a), as shown in Figure 16b, was created and resulted in a much improved first mode period of 0.33 s (same mode). Further, including a semi-rigid diaphragm (A1-3D-SD-a) brings the first mode period to 0.32 s. A key feature of the more detailed models are the inclusion of the full length ledger, or carrier, track, and the larger header members above openings. Proper inclusion of the gravity framing, even unsheathed, cuts the period in ½ and almost quadruples (4×!) the model stiffness. The engineering assumption of separation in response between the shear walls and gravity walls is false, even for the bare structural system. The experimental testing indicates that for the final building it is even more extreme: in the short direction the actual period (Phase 2e) is 0.26 s, a model based on shear wall only stiffness has a T=0.66 s, implying a nearly 7× difference in stiffness between a "reasonable" engineering assumption and the actual building.

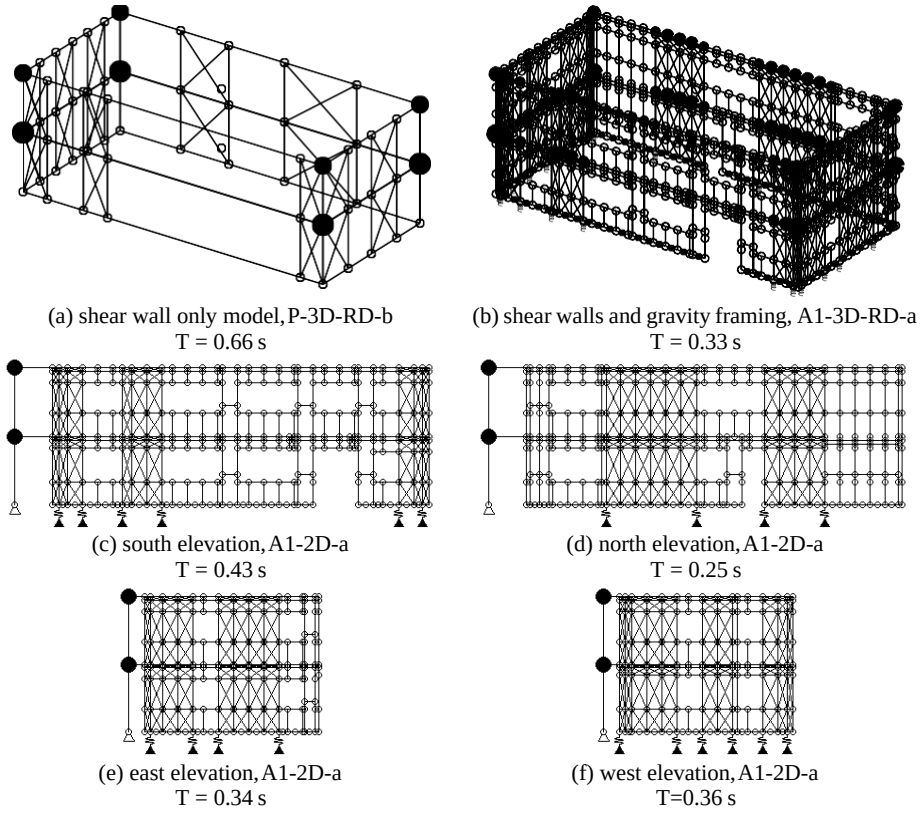

(a) shear wall only model, P-3D-RD-b
T = 0.66 s

(b) shear walls and gravity framing, A1-3D-RD-a
T = 0.33 s

(c) south elevation, A1-2D-a
T = 0.43 s

(d) north elevation, A1-2D-a
T = 0.25 s

(e) east elevation, A1-2D-a
T = 0.34 s

(f) west elevation, A1-2D-a
T=0.36 s

Figure 16: OpenSees models of the CFS-NEES Phase 1 archetype building
(note, (a) is graphically similar to A1-3D-RD-c except for hold down springs and shear anchors, (b) if the semirigid diaphragm is included per A1-3D-SD-a then T=0.32 s, and finally T=0.36 s in the test for Phase 1)

Extensive analysis has been conducted across the CFS-NEES model tree: linear static, vibration, nonlinear pushover, linear time history, and nonlinear time history analysis. The thesis by Leng [40] provides complete details; here, the focus is on the time history analysis. A condensed version of the results is provided in Table 3. Results are provided for the Phase 1, 100% Canoga Park excitation and for the Phase 2e, 100% Rinaldi excitation –see Section 7 for more details.

For the 100% Canoga Park excitation, the experimental response is summarized, along with experimental response predictions that are scaled from lower-level elastic tests (see first three rows of Table 3). The Phase 1 test, although returning to straight and having little visible damage (see [38] for more details), does experience inelastic deformations – approximately 25% increased drift and foundation forces. None of the state-of-the-practice (i.e., P) models (rows 4-7) provide meaningful predictions of the actual building response. The elastic P models have a grossly under-predicted stiffness, which for this model results in higher displacements, and the hysteretic P models (using Pinching4, but strength and stiffness based

on AISI S213 [5]) over-predict the drifts and forces by ~200 to 400%. The state-of-the-art (A) models have approximately the correct initial stiffness and thus the elastic model response has similar error to the elastic experimental response. The value of a 3D model is exhibited in the prediction of the hold-down forces – the 2D model over predicts the foundation demands. In general, the elastic A model is inadequate for safe prediction of the response. (Obviously, seismic response modification coefficients are used to correct such analyses when used in design, here the interest is in basic model performance). The nonlinear A models, utilizing calibrated Pinching4 shear wall models and the complete gravity framing system, perform reasonably well. The 2D A models over-predict drift by ~50% and the 3D A models by ~20% if the diaphragm is properly modeled. Foundation forces are over-predicted by ~25%. In general, the state-of-the art A models can reasonably represent the observed behavior in the Phase 1 testing.

Table 3: Summary Modeling options of CFS-NEES archetype building

Model Building Phase	Model State-of-	Model Type	Dim.	Floor, Roof Diaph.	Drift, long		Drift, short		Hold-down	Base shear		$\frac{\max\lvert\Delta u_{1,\text{long}}\rvert_{\text{model}}}{\max\lvert\Delta u_{1,\text{long}}\rvert_{\text{test}}}$	$\frac{\max\lvert\Delta v_{1,\text{short}}\rvert_{\text{model}}}{\max\lvert\Delta v_{1,\text{short}}\rvert_{\text{test}}}$	$\frac{F_{\text{HDmodel}}}{F_{\text{HDtest}}}$	ID[1]
					$\Delta u_1/h$ (%)	$\Delta u_2/h$ (%)	$\Delta v_1/h$ (%)	$\Delta v_2/h$ (%)	F_{HD} (kips)	$V_{b\text{-long}}$ (kips)	$V_{b\text{-short}}$ (kips)				
Phase 1/2a Building response, Canoga Park 100%, 3 directions, DBE level															
Experiment at 100% Canoga Park					1.18	0.81	0.85	0.56	9.8	-	-	**1.00**	**1.00**	**1.00**	P1S07
Experiment Scaled from Elastic					1.00	0.69	0.62	0.56	8.3	-	-	0.85	1.00	0.84	P1S04/0.16
Experiment Scaled from Elastic					0.88	0.75	0.62	0.56	7.8	-	-	0.93	1.00	0.79	P2aS04/0.16
1/2a	Practice	Elastic	2D	-	1.70	1.64	1.61	1.75	36.2	59.4	40.8	2.02	3.12	3.71	P-2D-b
1/2a	Practice	Elastic	3D	Rigid	1.83	1.68	2.03	-2.16	67.6	69.3	57.7	2.08	3.85	6.91	P-3D-RD-b
1/2a	Practice	Hyster.	2D	-	-3.96	-0.65	-4.39	-1.23	11.7	127	28.9	3.36	5.17	1.20	P-2D-b
1/2a	Practice	Hyster.	3D	Rigid	5.09	-0.78	-3.57	1.45	30.1	21.0	16.6	4.31	4.20	3.08	P-3D-RD-b
1/2a	Art	Elastic	2D	-	0.69	-0.45	-0.51	0.34	16.0	52.1	46.3	0.59	0.61	1.64	A1-2D-a
1/2a	Art	Elastic	3D	Rigid	-0.44	-0.31	-0.51	-0.35	8.7	53.9	51.7	0.38	0.63	0.89	A1-3D-RD-a
1/2a	Art	Elastic	3D	Semi.	-0.53	-0.21	0.53	0.30	8.1	48.8	58.1	0.45	0.63	0.83	A1-3D-SD-a
1/2a	Art	Hyster.	2D	-	1.81	0.52	1.26	-0.59	12.0	51.9	37.0	1.53	1.48	1.23	A1-2D-a
1/2a	Art	Hyster.	3D	Rigid	1.40	-0.69	1.15	0.68	12.6	46.4	39.1	1.19	1.36	1.29	A1-3D-RD-a
1/2a	Art	Hyster.	3D	Semi.	1.41	-0.53	0.90	0.33	11.8	51.5	41.5	1.19	1.06	1.21	A1-3D-SD-a
Phase 2e Building response, Rinaldi 100%, 3 directions, MCE level															
Experiment at 100% Rinaldi					0.67	0.45	0.72	0.99	7.6	-	-	**1.00**	**1.00**	**1.00**	P2eS09
Experiment Scaled from Elastic					0.69	0.44	1.00	0.69	2.9	-	-	1.03	1.39	0.39	P2eS08/0.16
1/2a	Practice	Elastic	2D	-	4.56	-4.18	-2.82	2.56	93.0	107	63.5	9.28	3.91	12.2	P-2D-b
1/2a	Practice	Elastic	3D	Rigid	3.17	-3.09	-3.12	-3.13	81.3	126	67.9	6.88	4.34	10.7	P-3D-RD-b
1/2a	Practice	Hyster.	2D	-	Analysis failed*							∞	∞	∞	P-2D-b
1/2a	Practice	Hyster.	3D	Rigid	12.14	9.14	-10.7	-3.96	38.8	21.9	18.6	20.3	14.9	5.10	P-3D-RD-b
1/2a	Art	Elastic	2D	-	1.14	0.75	1.34	0.88	24.7	92.2	119	1.71	1.85	3.25	A1-2D-a
1/2a	Art	Elastic	3D	Rigid	0.91	-0.62	1.17	0.72	25.3	117	117	1.39	1.63	3.33	A1-3D-RD-a
1/2a	Art	Hyster.	2D	-	Analysis failed*							∞	∞	∞	A1-3D-SD-a
1/2a	Art	Hyster.	3D	Rigid	Analysis failed*							∞	∞	∞	A1-3D-RD-a
2b	Art	Hyster.	3D	Rigid	1.85	-0.41	-1.01	-0.56	17.8	73.6	42.4	2.76	1.40	2.34	A2b-3D-RD-a
2c	Art	Hyster.	3D	Rigid	1.07	-0.37	1.04	0.57	16.2	84.0	53.2	1.59	1.45	2.14	A2c-3D-RD-a
2d	Art	Hyster.	3D	Rigid	0.84	-0.34	0.99	0.52	14.4	86.8	61.9	1.25	1.37	1.90	A2d-3D-RD-a
1/2a	Art	Hyster.	3D	Semi.	7.30	0.67	-1.19	-0.44	13.4	52.6	48.4	10.9	1.65	1.77	A1-3D-SD-a
2b	Art	Hyster.	3D	Semi.	1.64	0.33	1.20	0.38	17.5	77.1	53.5	2.45	1.66	2.31	A2b-3D-SD-a
2c	Art	Hyster.	3D	Semi.	1.01	0.25	1.16	0.37	15.3	85.1	64.0	1.51	1.61	2.01	A2c-3D-SD-a
2d	Art	Hyster.	3D	Semi.	Model not completed at this time										A2d-3D-SD-a

1: Experimental ID from [38] and Model ID from Table 2 and [40]
*: Displacements increase without bound during analysis

A benefit of having reasonable model confidence in the Phase 1 (state-of-the-art) modeling is the additional analysis that is possible from the model. For example, the predicted performance of selected shear walls during the 100% Canoga Park excitation is provided in Figure 17. In addition to demonstrating that the modeling of the shear wall into multiple panels(note the many diagonal truss elements in the shear wall of Figure 16 vs. Figure 16a) is working correctly, the results also indicate how much and which shear walls provide energy dissipation for the entire building. In addition, as provided in Figure 18, the foundation forces and the manner in which the base shear and compression/uplift is carried can be investigatedin detail. The three-dimensional nature of the response is highlighted by results such as Figure 18; however, the model does not appear to exhibit the same extent of coupling in the shearwall response as the tests (see Figure 14).

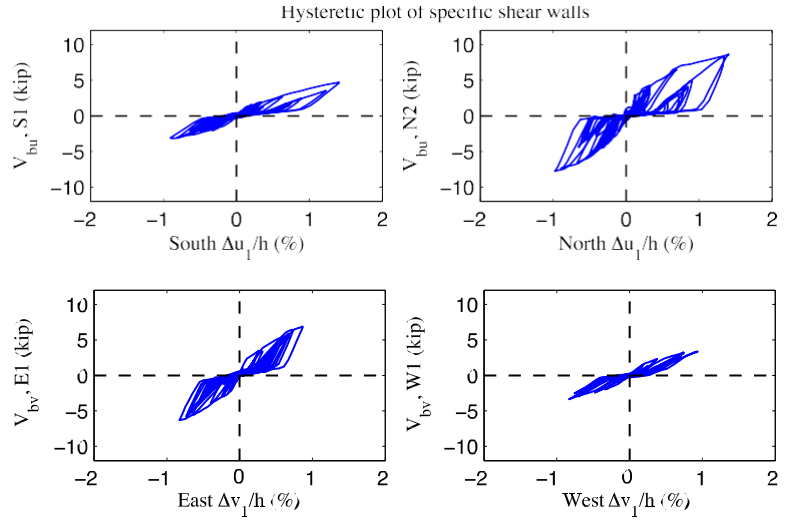

Figure 17: A1-3D-SD-a model, hysteretic plot of example shear walls at each elevation, 100 % Canoga Park, 3D nonlinear analysis

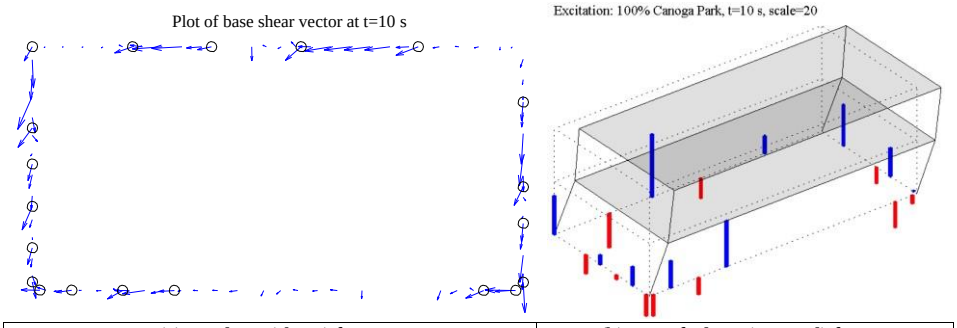

(a) in-plane (shear) force	(b) out-of-plane (vertical) forces

Figure 18: A1-3D-SD-a model, foundation forces, 100 % Canoga Park, 3D nonlinear analysis (maximum anchor/hold-down base shear is 2.35 kips)

Modeling the Phase 2 response of the building is more involved than Phase 1. Figure 19 provides a graphical depiction of the additional complexity that must be introduced into the model – including providing increased lateral stiffness to the gravity walls (note additional diagonal truss elements) first from exterior sheathing (phase 2b) then to all exterior walls when gypsum is installed on the interior face of the exterior walls (phase 2c). Stiffness predictions for these additions are based on the fastener-based model discussed in Section 6. Finally, the interior walls are introduced in the Phase 2d model, again with properties based on the fastener-based models of Section 6. The most advanced available model (A2d-3D-RD-a) has a first mode period of 0.22 s in the short direction and 0.17 s in the long direction, which may be compared with the experiment of 0.26 s in the short direction and 0.15 s in the long direction.

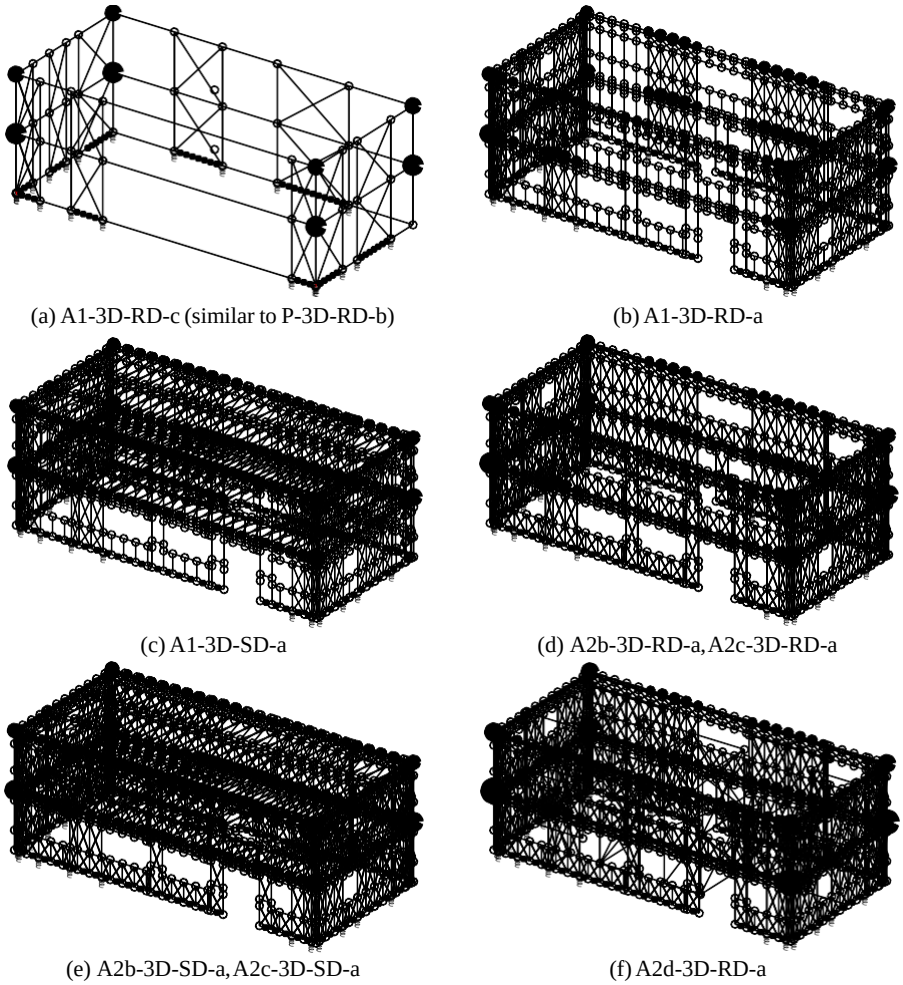

(a) A1-3D-RD-c (similar to P-3D-RD-b) (b) A1-3D-RD-a

(c) A1-3D-SD-a (d) A2b-3D-RD-a, A2c-3D-RD-a

(e) A2b-3D-SD-a, A2c-3D-SD-a (f) A2d-3D-RD-a

Figure 19: Example 3D OpenSees Models for Building Analysis

Elastic and nonlinear time history response of the OpenSees models with the Phase2e testing at an excitation of 100% Rinaldi is provided in the lower half of Table 3. The standard state-of-the-practice assumption that only the shear walls contribute in the lateral system, i.e. Figure 19a is grossly conservative. Essentially all of the state-of-the practice (P) models predict failure of the building due to excessive drift. That is, for a building that experienced no residual drift and only minor damage under an earthquake excitation consistent with the MCE level, even fairly robust P models predict building collapse.

The state-of-the-art (A) models fair better, though improvements are still needed. If the engineer chooses to model the full structural system – i.e. shear walls and gravity walls, but ignores all additional phases of construction, then the A1 or Phase 1/2a models result (Figure 19b or c). These A1 models are more accurate than the P models, but not accurate

enough to reasonably predict observed behavior. The inelastic time history analyses for the A1 models, whether 2D or 3D, predict excessive drift and collapse of the building, while in the actual response the building experiences less than 1% story drift. A conclusion to be drawn from this is that, in addition to the gravity walls, fire protection, exterior finish, and interior partitions also play a critical role in positively contributing to the observed, successful, lateral performance of the CFS-NEES building.

The state-of-the art model that includes construction through Phase 2d (A2d-3D-RD-a, Figure 19f) successfully predicts that the building will survive the Rinaldi 100% excitation and that story drifts in both the long and short directions will be less than 1%. The model over-predicts the peak story drift by ~30% and hold-down forces by ~100%. The overprediction of the hold down forces is non-trivial – it is clear that vertical load paths exist in the real structure that do not exist in the model. In particular, compression bearing paths from contact at the ends of all studs deserves further consideration. Additional analyses, including Incremental Dynamic Analysis, exploration of seismic response modification coefficients, and other details are provided in [40].

9 DISCUSSION

It is convenient and useful to separate the response of buildings, including cold-formed steel framed buildings, into lateral and gravity systems. By insuring at least one valid load path for both systems, the engineer hopes to ensure the building can survive actual loads. Further, it is equally useful to distinguish between structural systems and nonstructural additions to the structural systems (e.g. gypsum sheathing for fire protection) as well as structural systems and nonstructural systems, such as interior partition walls. An engineer has little control over these nonstructural details and systems, and a division of labor is beneficial to allowing other trades to assure overall building performance and function. However, the actual building response can vary significantly from the idealized structural system. In the CFS-NEES building the lateral stiffness of the building is increased 4× when the gravity systems contribution to the lateral system is considered, and another 4.5× when nonstructural details and systems are considered. In total, the actual building is 18× stiffer than an engineer's model based on the shear walls alone. The CFS-NEES building survived DBE and MCE excitations without permanent drift – a response that is as excellent as it is far from the assumed engineering behavior. The benefits of traditional design processes may be outweighed by the error in the approximation – examining whole building design will be necessary to capture the true response of these structures.

The CFS-NEES effort, combined with global efforts in cold-formed steel seismic design, are beginning to put the tools in place for needed whole building modeling. Efficient nonlinear hysteretic models for typical connections, cold-formed steel members, assemblages such as shear walls, gravity walls, trusses, etc. are all providing the needed building blocks. Modeling non-traditional and highly variable materials such as gypsum, including highly nonlinear load paths such as contact foundation conditions (bearing vs. uplift without a hold down), efficiently and accurately incorporating fundamentally thin-walled behavior such as unsymmetric open section torsion and cross-section buckling modes all present significant new challenges and much work remains to be done at both fundamental and practical levels. Improved models can assist in improved, or more thoroughly validated, seismic response modification coefficients (i.e. R, C_d, Ω_o in the U.S.), but also - and more importantly - open up pathways to whole building optimization. Although much work remains, the path forward seems reasonably clear, and the benefits significant; thus the author expects that research will

continue to advance towards useful whole building models for cold-formed steel framed buildings.

10 CONCLUSIONS

Seismic design of cold-formed steel framed buildings has advanced significantly and the recent North American CFS-NEES research effort has fully characterized expected system-level benefits for an archetypical building and provided tools for exploring these benefits in cold-formed steel buildings through efficient building-scale simulations. Current seismic design of cold-formed steel framed buildings relies largely on prescriptive shear wall capacity strength tables and assumed seismic response modification coefficients. The CFS-NEESeffort demonstrates that the current seismic methodology is conservative in an archetypical structure – but that current methods miss how such structures actually perform. Full-scale shake table testing, cyclic shear wall, member, and connection testing are all used to characterize the response of cold-formed steel framing. Phenomenological models for connections, members, and shear walls are all developed that may be efficiently used in full-scale building modeling. Taken together, the CFS-NEES effort is assisting in bringing state-of-the-art seismic performance-based design to cold-formed steel framed buildings. Significant work remains to fully translate the findings to practice, and to further advance the modeling tools to make whole building modeling for cold-formed steel framed buildings a more regular occurrence.

ACKNOWLEDGMENTS

The research team associated with the CFS-NEES project spanned multiple universities as well as consulting and industry. At Johns Hopkins University along with the author, faculty, graduate students, and visiting scholars including Naru Nakata, Kara Peterman, Jiazhen Leng, Matt Stehman, Peng Liu, Deniz Ayhan, and Cristina Gannea all contributed to the work as well as numerous undergraduate researchers. At Bucknell University faculty Steve Buonopane along with several undergraduate researchers led and contributed to several efforts. At Virginia Tech faculty Cris Moen and Matt Eatherton, along with graduate student David Padilla-Llanno contributed significantly to the effort through member and connection testing. At University of North Texas faculty Cheng Yu and at McGill University faculty Colin Rogers aided in several key areas. Devco Engineering through Rob Madsen provided significant design experience to the effort and was the chief designer of the CFS-NEES building. At the American Iron and Steel Institute, Bonnie Manley leads the seismic code team, and contributed throughout the life of the project.

All of these researchers, associated with the CFS-NEES project, would like to thank the National Science Foundation (NSF-CMMI #1041578), American Iron and Steel Institute (AISI), ClarkDietrich, Steel Stud Manufacturers Association, Steel Framing Industry Alliance, Devco Engineering, Mader Construction, DSi Engineering, Simpson Strong-Tie and the members of the Industrial Advisory Board: Renato Camporese, Thomas Castle, Kelly Cobeen, Randy Daudet, Richard Haws, Jay Parr, and Steven Tipping, as well as additional Industry Liaisons: George Frater, Don Allen, Tom Lawson, and Fernando Sessma. In addition, we would like to thank the team at the University of Buffalo SEESL facility, in particular Mark Pitman. The views expressed in this work are those of the authors and not NSF, AISI, or any of the participating companies, universities, or advisors.

Table 2: Modeling options of CFS-NEES archetype building

			State of the Practice				State of the Art										
							Phase 1/Phase 2a					Phase 2b			Phase 2c			Phase 2d
Component	Property	Option	P-2D-a	**P-2D-b**	P-3D-RD-a	**P-3D-RD-b**	**A1-2D-a**	**A1-3D-RD-a**	A1-3D-RD-b	A1-3D-RD-c	**A1-3D-SD-a**	A2b-2D-a	**A2b-3D-RD-a**	**A2b-3D-SD-a**	A2c-2D-a	**A2c-3D-RD-a**	**A2c-3D-SD-a**	**A2d-3D-RD-a**
Shear wall	Stiffness	$K(0.4V_{nP})$		**X**		**X**												
		$K(V_{nP})$	X		X													
		$K(0.2V_{nA})$					**X**	**X**		X	**X**	X	**X**	**X**	X	**X**	**X**	**X**
		$K(0.4V_{nA})$							X									

[1]Professor, Johns Hopkins University, <schafer@jhu.edu>

[2]Visiting Student Scholar, Johns Hopkins University

[3]Graduate Research Assistant, Johns Hopkins University

[4]Graduate Research Assistant, Virginia Polytechnic and State University

[5]Associate Professor, Bucknell University

[6]Assistant Professor, Virginia Polytechnic and State University

[7]Senior Project Engineer, Devco Engineering

[8]Regional Director, American Iron and Steel Institute

[9]Associate Professor, Virginia Polytechnic and State University

[10]Assistant Professor, Johns Hopkins University

[11]Professor, McGill University

[12]Associate Professor, University of North Texas

	Capacity	V_{nA}					X	X	X	X	X	X	X	X	X	X	X	X
		V_{nP}	X	X	X	X												
	Backbone	EPP	X		X													
		Pinching4		X		X	X	X	X	X	X	X	X	X	X	X	X	X
	Panel size	Whole	X	X	X	X				X								
		Subpanels					X	X	X		X	X	X	X	X	X	X	X
Hold-down	General	Smeared	X	X	X	X												
		Discrete					X	X	X	X	X	X	X	X	X	X	X	X
Shear anchors	General	Ignored	X	X	X	X												
		Included					X	X	X	X	X	X	X	X	X	X	X	X
Diaphragm	Stiffness	Flexible	X	X			X					X			X			
		Rigid			X	X		X	X	X			X			X		X
		Semi-rigid									X			X			X	
	Pinching	None	X	X	X	X	X	X	X	X		X			X			X
		Pinching4									X		X	X		X	X	
Gravity exterior walls	General	None	X	X	X	X				X								
		Frame					X	X	X		X							
		Full										X	X	X	X	X	X	X
Gypsum sheathing	General	Ignored	X	X	X	X	X	X	X	X	X	X	X	X				
		Included													X	X	X	X
Interior	General	Ignored	X	X	X	X	X	X	X	X	X	X	X	X	X	X	X	

walls		Included																				**X**
Mass distribution	General	Corner	X	**X**	X	**X**	**X**			X		X		X			X					
		Stud ends						**X**	X		**X**			**X**	**X**			**X**	**X**			**X**

Table 3: Summary Modeling options of CFS-NEES archetype building

Model Building Phase	Model State-of-	Model Type	Dim.	Floor, Roof Diaph.	Drift, long $\Delta u_1/h$ (%)	Drift, long $\Delta u_2/h$ (%)	Drift, short $\Delta v_1/h$ (%)	Drift, short $\Delta v_2/h$ (%)	Hold-down F_{HD} (kips)	Base shear $V_{b\text{-}long}$ (kips)	Base shear $V_{b\text{-}short}$ (kips)	$\frac{\max_{model}\lvert\Delta u_i\rvert}{\max\lvert\Delta u_i\rvert_{test}}$	$\frac{\max_{model}\lvert\Delta v_i\rvert}{\max\lvert\Delta v_i\rvert_{test}}$	$\frac{F_{HDmodel}}{F_{HDtest}}$	ID[1]
Phase 1/2a Building response, Canoga Park 100%, 3 directions, DBE level															
Experiment at 100% Canoga Park					1.18	0.81	0.85	0.56	9.8	-	-	**1.00**	**1.00**	**1.00**	P1S07
Experiment Scaled from Elastic					1.00	0.69	0.62	0.56	8.3	-	-	0.85	1.00	0.84	P1S04/0.16
Experiment Scaled from Elastic					0.88	0.75	0.62	0.56	7.8	-	-	0.93	1.00	0.79	P2aS04/0.16
1/2a	Practice	Elastic	2D	-	1.70	1.64	1.61	1.75	36.2	59.4	40.8	2.02	3.12	3.71	P-2D-b
1/2a	Practice	Elastic	3D	Rigid	1.83	1.68	2.03	-2.16	67.6	69.3	57.7	2.08	3.85	6.91	P-3D-RD-b
1/2a	Practice	Hyster.	2D	-	-3.96	-0.65	-4.39	-1.23	11.7	127	28.9	3.36	5.17	1.20	P-2D-b
1/2a	Practice	Hyster.	3D	Rigid	5.09	-0.78	-3.57	1.45	30.1	21.0	16.6	4.31	4.20	3.08	P-3D-RD-b
1/2a	Art	Elastic	2D	-	0.69	-0.45	-0.51	0.34	16.0	52.1	46.3	0.59	0.61	1.64	A1-2D-a
1/2a	Art	Elastic	3D	Rigid	-0.44	-0.31	-0.51	-0.35	8.7	53.9	51.7	0.38	0.63	0.89	A1-3D-RD-a
1/2a	Art	Elastic	3D	Semi.	-0.53	-0.21	0.53	0.30	8.1	48.8	58.1	0.45	0.63	0.83	A1-3D-SD-a
1/2a	Art	Hyster.	2D	-	1.81	0.52	1.26	-0.59	12.0	51.9	37.0	1.53	1.48	1.23	A1-2D-a
1/2a	Art	Hyster.	3D	Rigid	1.40	-0.69	1.15	0.68	12.6	46.4	39.1	1.19	1.36	1.29	A1-3D-RD-a
1/2a	Art	Hyster.	3D	Semi.	1.41	-0.53	0.90	0.33	11.8	51.5	41.5	1.19	1.06	1.21	A1-3D-SD-a
Phase 2e Building response, Rinaldi 100%, 3 directions, MCE level															
Experiment at 100% Rinaldi					0.67	0.45	0.72	0.99	7.6	-	-	**1.00**	**1.00**	**1.00**	P2eS09
Experiment Scaled from Elastic					0.69	0.44	1.00	0.69	2.9	-	-	1.03	1.39	0.39	P2eS08/0.16
1/2a	Practice	Elastic	2D	-	4.56	-4.18	-2.82	2.56	93.0	107	63.5	9.28	3.91	12.2	P-2D-b

1/2a	Practice	Elastic	3D	Rigid	3.17	-3.09	-3.12	-3.13	81.3	126	67.9	6.88	4.34	10.7	P-3D-RD-b
1/2a	Practice	Hyster.	2D	-	Analysis failed*							∞	∞	∞	P-2D-b
1/2a	Practice	Hyster.	3D	Rigid	12.14	9.14	-10.7	-3.96	38.8	21.9	18.6	20.3	14.9	5.10	P-3D-RD-b
1/2a	Art	Elastic	2D	-	1.14	0.75	1.34	0.88	24.7	92.2	119	1.71	1.85	3.25	A1-2D-a
1/2a	Art	Elastic	3D	Rigid	0.91	-0.62	1.17	0.72	25.3	117	117	1.39	1.63	3.33	A1-3D-RD-a
1/2a	Art	Hyster.	2D	-	Analysis failed*							∞	∞	∞	A1-3D-SD-a
1/2a	Art	Hyster.	3D	Rigid	Analysis failed*							∞	∞	∞	A1-3D-RD-a
2b	Art	Hyster.	3D	Rigid	1.85	-0.41	-1.01	-0.56	17.8	73.6	42.4	2.76	1.40	2.34	A2b-3D-RD-a
2c	Art	Hyster.	3D	Rigid	1.07	-0.37	1.04	0.57	16.2	84.0	53.2	1.59	1.45	2.14	A2c-3D-RD-a
2d	Art	Hyster.	3D	Rigid	0.84	-0.34	0.99	0.52	14.4	86.8	61.9	1.25	1.37	1.90	A2d-3D-RD-a
1/2a	Art	Hyster.	3D	Semi.	7.30	0.67	-1.19	-0.44	13.4	52.6	48.4	10.9	1.65	1.77	A1-3D-SD-a
2b	Art	Hyster.	3D	Semi.	1.64	0.33	1.20	0.38	17.5	77.1	53.5	2.45	1.66	2.31	A2b-3D-SD-a
2c	Art	Hyster.	3D	Semi.	1.01	0.25	1.16	0.37	15.3	85.1	64.0	1.51	1.61	2.01	A2c-3D-SD-a
2d	Art	Hyster.	3D	Semi.	Model not completed at this time										A2d-3D-SD-a

REFERENCES

[1] AISI S200 (2012). "North American Standard For Cold-Formed Steel Framing –General Provisions." American Iron and Steel Institute, Washington, DC.

[2] AISI S100 (2012). "North American Specification for the Design of Cold-Formed Steel Structural Members." American Iron and Steel Institute, Washington, DC.

[3] ECCS (2007). "Eurocode 3 – Design of steel structures – Part 1-3: General rules – Supplementary rules for cold-formed members and sheeting." ECCS.

[4] Serrette, R., Encalada, J., Juadines, M., and Nguyen, H. (1997). "Static Racking Behavior of Plywood, OSB, Gypsum, and FiberBoard Walls with Metal Framing." *Journal of Structural Engineering* 123 (8) 1079–1086.

[5] AISI S213 (2007). "North American Standard for Cold-Formed Steel Farming – Lateral Design." American Iron and Steel Institute, Washington DC. [Note 2012 Ed. also exists, AISI S400 will replace AISI S213 for seismic design in 2016].

[6] Branston, A., Chen, Y.C., Boudreault, F.A., Rogers, C.A. (2006). "Testing of Light-Gauge Steel-Frame – Wood Structural Panel Shear Walls." *Canadian Journal of Civil Engineering* 33 561–572. doi:10.1139/L06-014.

[7] Al-Kharat, M., Rogers, C.A. (2007). "Inelastic Performance of Cold-Formed Steel Strap Braced Walls." *Journal of Constructional Steel Research* 63 (4) 460-474.

[8] Balh, N., DaBreo, J., Ong-Tone, C., El-Saloussy, K., Yu, C., Rogers, C.A. (2014). "Design of Steel Sheathed Cold-Formed Steel Framed Shear Walls." *Thin-Walled Structures* 75 (February): 76–86. Doi:10.1016/j.tws.2013.10.023.

[9] Shamim, I., Dabreo, J., Rogers, C.A. (2013). "Dynamic Testing of Single- and Double-Story Steel-Sheathed Cold-Formed Steel-Framed Shear Walls." *Journal of Structural Engineering* 139 (5) 807-817.

[1]Professor, Johns Hopkins University, <schafer@jhu.edu>

[2]Visiting Student Scholar, Johns Hopkins University

[3]Graduate Research Assistant, Johns Hopkins University

[4]Graduate Research Assistant, Virginia Polytechnic and State University

[5]Associate Professor, Bucknell University

[6]Assistant Professor, Virginia Polytechnic and State University

[7]Senior Project Engineer, Devco Engineering

[8]Regional Director, American Iron and Steel Institute

[9]Associate Professor, Virginia Polytechnic and State University

[10]Assistant Professor, Johns Hopkins University

[11]Professor, McGill University

[12]Associate Professor, University of North Texas

[10]Yu, C. (2010). "Shear Resistance of Cold-Formed Steel Framed Shear Walls with 0.686 mm, 0.762 mm, and 0.838 mm Steel Sheet Sheathing." *Engineering Structures* 32 (6) 1522-1529.

[11]Landolfo, R., Fiorino, L., and Della Corte, G. (2006). "Seismic Behavior of Sheathed Cold-Formed Structures: Physical Tests." *Journal of Structural Engineering* 132 (4) 570-581.

[12] Fiorino, L., Della Corte, G., Landolfo, R. (2007). "Experimental tests on typical screw connections for cold-formed steel housing." *Engineering Structures* 29 (8) 1761-1773.

[13]Iuorio, O., Fiorino, L., Landolfo, R. (2014). "Testing CFS Structures: The New School BFS in Naples." *Thin-Walled Structures* 84:275-288.

[14]Fiorino, L., Iuorio, O., Landolfo, R. (2009). "Sheathed Cold-Formed Steel Housing: A Seismic Design Procedure." *Thin-Walled Structures* 47 (8-9): 919-930.

[15]Fülöp, L. A., Dubina, D. (2006). "Design Criteria for Seam and Sheeting-to-Framing Connections of Cold-Formed Steel Shear Panels." *Journal of Structural Engineering* 132 (4): 582-590.

[16] Fülöp, L. A., Dubina, D. (2004). "Performance of Wall-Stud Cold-Formed Shear Panels Under Monotonic and Cyclic Loading - Part II: Numerical Modelling and Performance Analysis." *Thin-Walled Structures* 42 (2)339-349.

[17]Dubina, D. (2008). "Behavior and Performance of Cold-Formed Steel-Framed Houses Under Seismic Action." *Journal of Constructional Steel Research* 64 (7-8) 896-913.

[18]Gad, E.F., Duffield, C.F., Hutchinson, G.L., Mansell, D.S., Stark, G. (1999). "Lateral Performance of Cold-Formed Steel-Framed Domestic Structures." *Engineering Structures* 21 (1) 83-95.

[19] Li, Y., Shen, S., Yao, X., Ma, R., Liu, F. (2012). "Experimental Investigation and Design Method Research on Low-Rise Cold-Formed Thin-Walled Steel Framing Buildings." *Journal of Structural Engineering* 818–836. doi:10.1061/(ASCE)ST.1943-541X.0000720.

[20] AISI S400 (2015). "North American Standard for Seismic Design of Cold-Formed Steel Structural Systems." American Iron and Steel Institute, Washington, DC.

[21] Madsen, R.L., Nakata, N., Schafer, B.W. (2011). "CFS-NEES Building Structural Design Narrative", Research Report, RR01, access at www.ce.jhu.edu/cfsness, October 2011, revised RR01b April 2012, revised RR01c May 2012.

[22] Nakata, N., Schafer, B.W., Madsen, R.L. (2012). "Seismic Design of Multi-Story Cold-Formed Steel Buildings: the CFS-NEES Archetype Building," 2012 Structures Congress, March 2012, Chicago, Illinois. 1507-1517.

[23] Ayhan, D., Schafer, B.W. (2012). "Moment-Rotation Characterization of Cold-Formed Steel Beams" Research Report, CFS-NEES, RR02, April 2012, access at www.ce.jhu.edu/cfsnees.

[24] Ayhan, D., Schafer, B.W. (2011). "Impact of cross-Section stability on cold-formed steel member stiffness and ductility", Annual Stability Conference, Structural Stability Research Council, May 10-14 2011, Pittsburgh, PA.

[25] Ayhan, D., Schafer, B.W. (2012). "Characterization of moment-rotation response of cold-formed steel beams", Annual Stability Conference, Structural Stability Research Council, April 2012, Grapevine, Texas.

[26] Ayhan, D., Schafer, B.W. (2012). "Moment-Rotation Characterization of Cold-Formed Steel Beams Depending on Cross-Section Slenderness" 15th World Conference on Earthquake Engineering, September 24-28, Lisbon, Portugal.

[27] Liu, P., Peterman, K.D., Schafer, B.W. (2012). "Test Report on Cold-Formed Steel Shear Walls" Research Report, CFS-NEES, RR03, June 2012, access at www.ce.jhu.edu/cfsnees

[28] Liu, P., Peterman, K.D., Yu, C., Schafer, B.W. (2012). "Cold-formed steel shear walls in ledger-framed buildings", Annual Stability Conference, Structural Stability Research Council, April 2012, Grapevine, Texas.

[29] Liu, P., Peterman, K.D., Yu, C., Schafer, B.W. (2012). "Characterization of cold-formed steel shear wall behavior under cyclic loading for the CFS-NEES building." Proc. of the 21st Int'l. Spec. Conf. on Cold-Formed Steel Structures, 24-25 October 2012, St. Louis, MO, 703-722.

[30] Folz, B., Filiatrault, A. (2001). Cyclic analysis of wood shear walls. *Journal of Structural Engineering* 2001; 127(4): 433-441.

[31] Lowes, L., Mitra, N., Altoontash, A. (2004). A Beam-Column Joint Model for Simulating the Earthquake Response of Reinforced Concrete Frames. PEER Rep. 2003/10, www.peer.berkeley.edu. [Source for Pinching04 Model in OpenSees]

[32] Peterman, K.D., Schafer, B.W. (2013). "Hysteretic shear response of fasteners connecting sheathing to cold-formed steel studs" Research Report, CFS-NEES, RR04, January 2013, access at www.ce.jhu.edu/cfsnees

[33] Peterman, K.D., Nakata, N., Schafer, B.W. (2012). "Cyclic Behavior of Cold-Formed Steel Stud-to-Sheathing Connections" 15th World Conference on Earthquake Engineering, September 24-28, Lisbon, Portugal.

[34] Padilla-Llano, D., Moen, C.D., Eatherton, M.R. (2014). Energy dissipation of cold-formed steel connections. Final Report, American Iron and Steel Institute, Washington, D.C.

[35] Buonopane, S.G, Tun, T.H., Schafer, B.W. (2014). Fastener-based computational models for prediction of seismic behavior of CFS shear walls. *Proceedings of the 10th National Conference in Earthquake Engineering*, Earthquake Engineering Research Institute, Anchorage, AK.

[36] Buonopane, S.G., Bian, G., Tun, T.H., Schafer, B.W. (2015). "Computationally efficient fastener-based models of cold-formed steel shear walls with wood sheathing." *Journal of Constructional Steel Research* 110 (2015) 137–148.

[37] Bian, G., Padilla-Llano, D.A., Buonopane, S.G., Moen, C.D., Schafer, B.W. (2015). "OpenSees modeling of wood sheathed cold-formed steel framed shear walls." *Proceedings of the Annual Stability Conference*, Structural Stability Research Council, Nashville, Tennessee, March 24-27, 2015, 14pp.

[43] Bian, G., Padilla-Llano, Leng J., D.A., Buonopane, S.G., Moen, C.D., Schafer, B.W. (2015) "OpenSees modeling of cold-formed steel framed gravity walls." *Proceedings of the 8th International Conference on Behavior of Steel Structures in Seismic Areas*, 1-4 July, Shanghai, China.

[38] Peterman, K.D., (2014). Behavior of full-scale cold-formed steel buildings under seismic excitations. Ph.D. Dissertation. Johns Hopkins University, Baltimore, Maryland May 2014

[39] ASCE 7-05 (2005)."Minimum Design Loads for Buildings and Other Structures." 2005 edition. American Society of Civil Engineers [The CFS-NEES building also references ASCE 7-10, and the current version is ASCE 7-15]

[40] Leng, J. (2015). Simulation of cold-formed steel structures. Ph.D. Dissertation. Johns Hopkins University, Baltimore, Maryland, Forthcoming: Summer 2015.

[41] Leng, J., Schafer, B.W., Buonopane, S.G. (2013). "Modeling the seismic response of cold-formed steel framed buildings: model development for the CFS-NEES building." Proc. of the Annual Stability Conference - Structural Stability Research Council, St. Louis, MO, April 16-20, 2013, 17pp.

[42] Leng, J., Schafer, B.W., Buonopane, S.G. (2012). "Seismic Computational Analysis of CFS-NEES Building." Proc. of the 21st Int'l. Spec. Conf. on Cold-Formed Steel Structures, 24-25 October 2012, St. Louis, MO,801-820.

[48] Peterman, K. D., Stehman, M. J. J, Madsen, R. L., Buonopane, S. G., Nakata, N., Schafer, B. W. (2016) "Experimental Seismic Response of a Full-Scale Cold-Formed Steel Framed Building: System-level Response" *Journal of Structural Engineering* [in press].

[49] Peterman, K. D., Stehman, M. J. J, Madsen, R. L., Buonopane, S. G., Nakata, N., Schafer, B. W. (2016) "Experimental Seismic Response of a Full-Scale Cold-Formed Steel Framed Building: Component-level Response" *Journal of Structural Engineering* [in press].